A locomotor assay reveals deficits in heterozygous Parkinson's disease model and proprioceptive mutants in adult *Drosophila*

Aman Aggarwal[a,b,1], Heinrich Reichert[c,2], and K. VijayRaghavan[a,1]

[a]National Centre for Biological Sciences, Tata Institute of Fundamental Research, Bangalore 560065, Karnataka, India; [b]Manipal Academy of Higher Education, Manipal 576104, Karnataka, India; and [c]Biozentrum, University of Basel, 4056 Basel, Switzerland

Contributed by K. VijayRaghavan, October 14, 2019 (sent for review May 2, 2018; reviewed by Pavan Ramdya and Darren W. Williams)

Severe locomotor impairment is a common phenotype of neurodegenerative disorders such as Parkinson's disease (PD). *Drosophila* models of PD, studied for more than a decade, have helped in understanding the interaction between various genetic factors, such as *parkin* and PINK1, in this disease. To characterize locomotor behavioral phenotypes for these genes, fly climbing assays have been widely used. While these simple current assays for locomotor defects in *Drosophila* mutants measure some locomotor phenotypes well, it is possible that detection of subtle changes in behavior is important to understand the manifestation of locomotor disorders. We introduce a climbing behavior assay which provides such fine-scale behavioral data and tests this proposition for the *Drosophila* model. We use this inexpensive, fully automated assay to quantitatively characterize the climbing behavior at high parametric resolution in 3 contexts. First, we characterize wild-type flies and uncover a hitherto unknown sexual dimorphism in climbing behavior. Second, we study climbing behavior of heterozygous mutants of genes implicated in the fly PD model and reveal previously unreported prominent locomotor defects in some of these heterozygous fly lines. Finally, we study locomotor defects in a homozygous proprioceptory mutation (*Trp-γ*^{1}) known to affect fine motor control in *Drosophila*. Moreover, we identify aberrant geotactic behavior in *Trp-γ*^{1} mutants, thereby opening up a finer assay for geotaxis and its genetic basis. Our assay is therefore a cost-effective, general tool for measuring locomotor behaviors of wild-type and mutant flies in fine detail and can reveal subtle motor defects.

Drosophila | climbing | locomotion | Parkinson's | geotaxis

Movement in living beings, such as locomotion, is the output of the nervous system (1). It entails not only properly functional body structures but also the neuronal mechanisms giving the output and processing information from various sensory modalities. Locomotion has been studied in detail for decades in a multitude of organisms ranging from simple to complex. A fine control of neuronal activity in a well-orchestrated manner has been shown to be necessary for proper locomotor output. The slightest disruption in this regulation can be highly detrimental to the animal's ability to move its limbs in a coordinated fashion.

In *Drosophila*, negative geotaxis is an intricate part of its locomotor behavior and has been studied for over a century (2). Climbing assays were used to identify and study molecules involved in fly models of fine motor control (3), Alzheimer's disease (4), Parkinson's disease (PD) (5), aging (6) and motor function degenerative disorders such as spinal muscle atrophy (7). Although these studies unveiled a plethora of valuable information, one major aspect which was overlooked was that all these results were based on mechanical stimulation of the flies. For example, most of the common climbing assays employ tapping down of the flies onto the hard glass/polystyrene surface of test tubes (6, 8). This regime of coercing flies to the bottom of the test tubes, although very effective, could induce physical stress and trauma to the flies (9). Since exposure to physical stress can alter the behavioral output of an animal, assays implementing tapping of flies could miss out on fine locomotor differences, if not the most prominent ones.

In his classical work, Carpenter (2) studied various combinations of phototaxis and geotaxis in flies. He postulated that light induces locomotion whereas gravity induces directionality in freely moving flies. Positive phototaxis with regard to negative geotaxis has been further studied in the countercurrent assay by the Benzer and other laboratories, with mechanical agitation being an intricate part of these assays (8, 10). Mechanical stimulation could be a deterrent in the accurate measurement of behavior. Carpenter used mechanical stimulation only when flies showed little to no locomotion. Flies show bouts of activity interspersed with nonactive periods, resulting in activity duration of not more than 40% of the total time (11). Thus, an assay which can measure locomotor activity in flies without any forceful artificial stimulation could be useful in tracking even subtle behavioral differences.

Multiple behavioral assays were developed decades ago to assay negative geotactic behavior of flies, ranging from the simplistic flies in a cylinder (2) to a countercurrent rapid iterative negative geotaxis assay (8) and geotaxis maze (12). However, there has not been any significant advancement in climbing behavior assays since then. Traditionally, fly climbing assays have been manual and

Significance

Fine control of neuronal activity is required for proper motor output. Severe locomotor impairment is a common result of neurodegenerative disorders such as Parkinson's disease (PD). The fruit fly, *Drosophila*, has been widely used as a model system to study the genetics of these disorders and simple climbing assays have been used to study the behavioral phenotypes of mutations in these genes. Here we introduce a fully automated climbing behavior assay and characterize climbing behavior in adults of various fly lines, including a proprioceptive mutant and different PD model flies, at high parametric resolution using this assay. Our assay is a general tool for measuring locomotor behavior of flies in fine detail and can reveal very subtle defects.

Author contributions: A.A. and K.V. designed research; A.A. performed research; A.A. contributed new reagents/analytic tools; A.A., H.R., and K.V. analyzed data; and A.A., H.R., and K.V. wrote the paper.

Reviewers: P.R., École Polytechnique Fédérale de Lausanne; and D.W.W., King's College London.

The authors declare no competing interest.

Data deposition: The software for data acquisition and analysis along with all the digitized raw data are available at https://gitlab.com/amanaggarwal/fly-vrl.

[1]To whom correspondence may be addressed. Email: amanaggarwal@ncbs.res.in or vijay@ncbs.res.in.

[2]Deceased June 13, 2019.

This article contains supporting information online at https://www.pnas.org/lookup/suppl/doi:10.1073/pnas.1807456116/-/DCSupplemental.

First published November 20, 2019.

labor-intensive where the climbing behavior is scored by keeping track of the flies visually and scoring for a minimum distance climbed in a fixed time duration (10). Along with being time-consuming, these assays inadvertently introduce inconsistency in the results. A mechanized system with minimal human intervention for measuring the behavior would be ideal for getting robust and consistent behavioral output. Not only could the measuring apparatus be automated but data analysis could also be computerized, thus making the output even more reliable and alleviating the need for countless hours of manually keeping track and timings of the flies. Here we describe "fly vertically rotating arena for locomotion" (fly-VRL), an assay for fly climbing behavior which does not cause mechanical agitation and is automated for behavior and data analysis. We used this fully automated assay to quantitatively characterize climbing behavior at high parametric resolution in wild-type flies as well as in 2 mutant contexts: mutants of genes implicated in the fly PD model and a mutant in proprioceptory structures.

The *parkin*, PINK1, and LRRK genes are some of the most rigorously studied genes in various fly models of PD. Mutations in *parkin* and PINK1 are known to be autosomal-recessive while a mutant LRRK gene is known to cause late-onset autosomal-dominant PD (13, 14). Heterozygous mutations in *parkin* and PINK1 genes are thought to enhance the risk for PD early onset (13). Here, we use $park^{25}$/+ flies to test climbing specifically in heterozygous *parkin* mutants and we also test a commonly used experimental control $PINK1^{RV}$ which is a revertant allele for PINK1 mutation (15). Mutations in LRRK are one of the strongest risk factors in sporadic PD (14). Studies in flies involving the LRRK gene have looked at behavioral manifestations of the PD phenotype in homozygous condition. We examined the behavior of heterozygous $LRRK^{ex1}$/+ mutants and studied the effect of $park^{25}$ mutations in transheterozygous state with $LRRK^{ex1}$ mutation. Behavioral phenotypes in these PD fly models were not reported for early-stage adult heterozygous flies and using our newly developed assay we observed significant differences in behavioral phenotypes in these fly models of PD at early adult stage in their life cycle.

Further, to test the sensitivity of this assay to reveal subtle changes in climbing abilities of the flies, we studied the climbing locomotor behavior of a proprioceptory mutant, $Trp\text{-}\gamma^{1}$. Trp-γ is a TRPC channel which is known to be expressed in mechanosensory neurons of thoracic bristles and the femoral chordotonal organ. The $Trp\text{-}\gamma^{1}$ mutant has defects in fine motor control but otherwise no major locomotor defects (3). We identified aberrant geotactic behavior in $Trp\text{-}\gamma^{1}$ mutants, thereby opening up a finer assay for geotaxis and its genetic basis in flies.

Materials and Methods

Fly Culturing. Flies were grown at 23 °C with a 12-h/12-h light/dark cycle. One-day-old flies were collected and both-sex cohorts were maintained on standard corn meal agar vials for the assay. Climbing behavior was performed on 3- to 5-d-old flies. *Canton-S* (CS) flies were used as wild type. CS, w^{1118};;, $PINK1^{RV}$;;, w^{1118};;Trp-γ^{1}, and w*;;$LRRK^{ex1}$/TM6b,Tb flies were obtained from Bloomington *Drosophila* Stock Center. w^{-};;$park^{25}$/TM3-Ser flies are used as described already (16). Males from w^{-};;$park^{25}$/TM3-Ser and w*;;$LRRK^{ex1}$/TM6b,TB were crossed with virgin females of w^{1118};; to generate w^{1118};;$park^{25}$/+ and w*;;$LRRK^{ex1}$/+ flies, respectively. Transheterozygote flies of genotype w*;;$LRRK^{ex1}/park^{25}$ were obtained by crossing males of w*;;$LRRK^{ex1}$/TM6B,Tb with virgin females from w^{-};;$park^{25}$/TM3-Ser.

Climbing Setup. The behavior cassette (Fig. 1*B*) design is modified from a previously published design (17) and was custom-built with 3 sections, top, middle, and bottom, which were held together with 4 screws. The top and middle section were fabricated using transparent acrylic sheet of 3-mm thickness. A 6-mm-diameter circular hole was drilled in the top section for introducing flies into the cassette. The middle section contained a 110- × 10- × 3-mm (length × breadth × height) slot which was used as climbing arena for the flies. The bottom section was made of translucent white acrylic sheet to act as a diffuser for the background light for uniform illumination.

Backlight: The behavior cassette was uniformly illuminated from the back using a custom-built infrared (IR) light source. The IR light source was built using 8 IR light-emitting diodes (LEDs) (SFH4550; Osram) connected in series and powered by a standard 15-V switch-mode power supply using current controlled circuit. A custom-built light guide panel system was used to provide uniform illumination to the climbing arena.

Vertical rotation mechanism: The climbing behavior setup is based on the vertical rotation of the behavior cassette. An Arduino controlled servo motor (S3003; Futaba)-based mechanism was implemented for vertical rotation (in one plane) of the behavior cassette. The servo rotates at 180 rpm with a stationary period of 15 s per 180° of rotation. The rotation speed of the arena is extremely slow as compared to a fly's turning speed (18). The backlight and the behavior cassette are mounted on the servo motor using a retractable 50- × 35-mm custom-made clamp. The retractable clamp provides the ability to quickly disengage the cassette from the rotation mechanism for changing.

Arena Details. A sliding mechanism in the behavior cassette allows the fly entry slot to be superimposed on the climbing arena. A single fly is gently

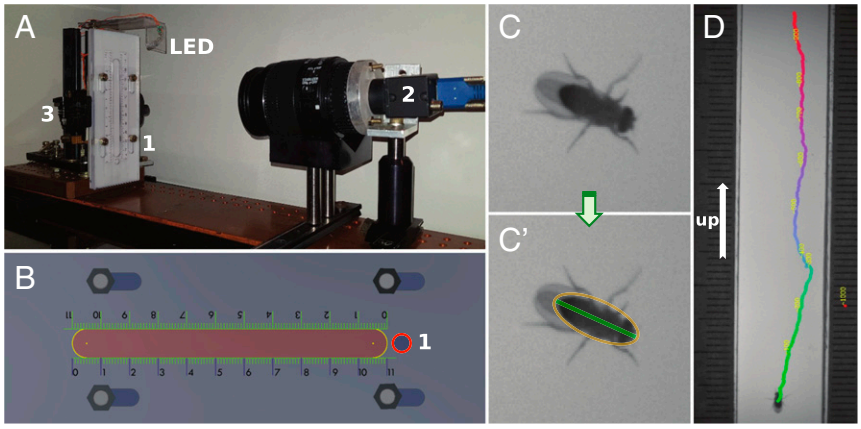

Fig. 1. Fly climbing setup. (*A*) Actual image of the fly climbing experimental setup consisting of a climbing cassette (*1*), camera (*2*), cassette rotating mechanism (*3*), and an ultraviolet LED light. (*B*) Schematic of the behavior cassette in which 1 depicts the hole from where the experimental fly is introduced into the climbing arena. (*C*) Top view of a wild-type CS male *Drosophila* during one of the recorded climbings. (*C′*) Representative segmentation of the same fly in the same video frame, with the orange oval representing the automatically detected body contour and green line depicting fly body length. (*D*) Raw frame of a fly climbing up in the arena, superimposed with its track after post hoc calculation by FlyConTra software. The green-to-red color map indicates the position of the fly during the track, with green and red indicating the start and end position of the fly, respectively. Numbers in yellow represent the frame number with respect to the position of the fly in the track, detected by FlyConTra, at that particular time point (Movie S1).

tapped into the climbing arena from the fly vial without anesthesia. Further, the behavior cassette is clamped to the servo to allow vertical rotation of the cassette. The assay is started soon after the fly's entry into the arena.

Image Capturing. Fly behavior is captured at 250FPS using a Pointgrey camera (13Y3M) with a Canon 18–55ES lens at 55-μm-per-pixel resolution. The lens aperture is maximized to increase light capture. The depth of field of the lens assembly allows capturing good-resolution images of a fly climbing on either the top or bottom section of the arena. A constant area of the arena, 70 × 10 mm, was imaged, which enabled analysis of the climbing behavior at high spatiotemporal resolution.

FlyConTra Software.

Data capturing. Imaging is done using a custom FlyConTra (Fly Contour-based Tracker) program, written in Python, which employs motion detection for image capturing. Image capturing is started immediately after the cassette is clamped on to the rotation assembly. Motion detection in FlyConTra initiates image capturing if there is any movement, within the defined thresholds, in the arena being filmed. Algorithms deployed in FlyConTra help in capturing images only when the fly is moving in a stationary arena, thus minimizing the amount of data captured. Image analysis for fly climbing behavior is done by FlyConTra post hoc.

Image analysis. FlyConTra detects the fly based on its shape and contrast with the background, similar to a method described by Branson et al. (19), but written in open source Python. Parameters defining the body shape and contrast can be adjusted in the software for rough approximation of fly shape. FlyConTra calculates the exact fly shape parameters for each fly by analyzing the dataset of that fly. The fly is detected in each frame and the coordinates of its position in sequential frames are saved in a corresponding file. This positional information is then used to calculate the further climbing parameters such as average speed, number of tracks, distance traveled, and various other parameters.

Parameters Calculated. We used fly track as a basic unit to measure locomotion of flies in the arena. A track is defined as the path treaded by a fly when it moves continuously for a distance greater than one body length unit (BLU) without stopping for more than one-fifth of a second at a time. For example, if a fly with BLU ~ 2.53 mm moves a distance of 15 mm, but stops for 0.3 s after moving 9 mm, FlyConTra would calculate that as 2 tracks. The following parameters of fly locomotion were calculated from the data captured from various flies of a given strain.

Total number of tracks. Total number of tracks of a genotype in a given time duration is the mean of number of tracks climbed by each fly of that genotype.

Total distance traveled. Distance traveled by a fly is equal to the sum of all track lengths in BLUs in a given time duration. For a genotype, total distance traveled in a given time is calculated as the mean of total distance traveled by each fly of that genotype.

Track duration. Duration of a track is the median of the duration, in seconds of each track, once the fly initiates movement. For a genotype, the duration of tracks, in a given time, is calculated by taking the mean of median track duration of each fly of that genotype.

Average speed. For each track, the speed of the fly is calculated as the average instantaneous speed for that track. Further, the mean speed of a fly is given by the mean of speeds for all tracks. Finally, for a genotype, average speed is calculated as the mean of mean speed of each fly.

Average track straightness. The track straightness is the coefficient of determination, r^2 value, of the linear regression model of the fly position in a track. For a genotype, the average track straightness is calculated as the mean of coefficient of determination of all tracks of a fly.

Geotactic index. The geotactic index (GTI) is the measure of a fly's ability to sense and act apropos of gravity. Each track in which the fly moves against gravity (from the bottom toward the top of the arena) is scored −1. Similarly, each track where a fly moves along gravity (from the top to bottom of the arena) is scored +1. Tracks where the fly does not show any vertical displacement above given threshold, are scored zero (0). GTI is calculated as

$$\text{Geotactic index} = \left(\Sigma T_{up} + \Sigma T_{down}\right) / \left(\Sigma T_{up} - \Sigma T_{down} + \Sigma T_{None}\right),$$

where ΣT_{up} is total score of all tracks against gravity, ΣT_{down} is total score of all tracks along gravity, and ΣT_{None} is total score of tracks without any vertical displacement.

Gait Analysis. The lens was adjusted for 27.5-μm-per-pixel resolution and video was captured at 250 frames per second (FPS). A constant area, 35 × 10 mm, of the arena was imaged for measuring gait pattern of the flies. Parts of the tracks with straight runs were sorted. Leg tips were detected using a modified version of the previously published rat-tail algorithm (20) following which the gait pattern was calculated. Briefly, the images of a straight run of a fly were manually selected, followed by background subtraction. Next, the fly contour was detected using binary thresholding and a body-centric stack was generated. Further, the fly body contour was detected by first eroding the thresholded fly contour 2 times, then dilating the leftover contour twice. Finally, leg contours were obtained by subtracting the fly body contour from the whole fly contour. Leg tips were calculated as the point farthest on the leg contour from the centroid of the fly. Leg tips were further clustered semiautomatically using spectral clustering and then manually assignment of clusters to the individual legs. Missed leg tip detections were calculated by interpolating the previous and the latest detection by a straight path (*SI Appendix*, Fig. S3).

Statistical Analyses. Statistical analyses of all raw data were done in Python and R. Graphs were plotted using matplotlib library in Python. For comparison between 2 genotypes, unpaired *t* test (for normal distribution) or Mann–Whitney *U* test (for nonnormal distribution) was used. For comparison between more than 2 genotypes, one-way ANOVA followed by Tukey's post hoc test (for normal distribution) or Kruskal–Wallis test followed by Dunn's post hoc test (for nonnormal distribution) was used. For time series data, longitudinal data analysis, for nonnormal data implemented in the R statistical package *nparLD* (21) was used, followed by post hoc analysis using the nparcomp package (22). The multiple contrasts test procedures (MCTP) function used for post hoc analysis from the nparcomp package corrects for familywise type I error rate (FWER). Numerical data are reported as mean ± SEM.

Software and Data Availability. The latest version of FlyConTra software and raw digitized data from the video files can be downloaded from: https://gitlab.com/amanaggarwal/fly-vrl. Readers may contact the authors directly for raw video files.

Results

Automated Analysis of Locomotor Climbing Behavior in *Drosophila*. Advances in image capturing and analysis techniques during the last couple of decades have made it possible to obtain detailed quantitative insights into many aspects of fly locomotor behavior. Using digital, high-speed image capturing technology and analysis we developed an automated assay which gives us information on fly climbing behavior with high parametric resolution (Fig. 1*A*). The setup consists of a fly behavior cassette (Fig. 1*B*) mounted on an automatically rotated cassette holder. The arena, big enough for a fly to move freely (110 × 10 × 3 mm; Fig. 1*B*), was carved inside the behavior cassette and mounted on an automated servo motor. The servo (Fig. 1*A*), controlled electronically, gives flies 15 s per rotation to climb in the arena (Movie S1). The rotation speed of the arena was not more than 60° per second, much less than a fly's turning speed (18). The arena was uniformly backlit via IR light, enabling imaging of freely moving flies in a well-illuminated space. An ultraviolet LED was placed toward the top of the cassette (Fig. 1*A*). Single fly behavior was recorded for at least 5 min for multiple rotations per fly via imaging and analyzed by tracking the fly in the images (Fig. 1*C*). The fly was detected on the basis of its body's elliptical shape along with contrast from the background using custom-developed FlyConTra software (Fig. 1*C′*). Fly track, the basic unit to define the locomotor behavior of the flies, is defined as the path treaded by the fly when it moves more than one body length continuously without stopping for more than 0.2 s at a time (Fig. 1*D* and Movie S2). Fly locomotor parameters were calculated from the tracks recorded. Fly behavior parameters were analyzed on a per-minute basis as well as for a total of 5 min to assess the fly activity bouts, which also depend upon the time spent in a new arena (11). Time series analysis of locomotion parameters enable us to compare fly behavior as the fly starts to acclimatize in the arena.

Locomotion Parameters of Climbing Wild-Type Flies. In order to validate our automated image capturing and analysis setup of a fly in the climbing arena and establish locomotor baseline parameters

for further studies with mutants, we first determined the locomotion parameters of climbing wild-type flies. In this validation study the following climbing parameters were characterized: number of tracks, average track duration, total distance traveled, average speed, and path straightness.

Number of tracks. The number of tracks climbed by flies is the direct measure of locomotor behavior. To estimate the motivation to climb, the total number of tracks were quantified for each fly. Climbing for 38 CS flies was measured. The behavior cassette rotates at 3.33 rpm, a total of around 17 times in 5 min (Fig. 2*A*). CS flies climbed 3.97 ± 0.18 tracks (mean ± SEM) in the first minute and gradually slowed down to a minimum of 3.23 ± 0.13 tracks per minute in the fourth minute (Fig. 2*A′* and Dataset S1). The slight but significant decrease in locomotion could be attributed to the fly's acclimatization to the arena. Overall, wild-type flies walked for 18.32 ± 0.44 tracks in the first 5 min after they were introduced in the climbing arena (Fig. 2*A* and Dataset S1). The average number of tracks climbed by the wild-type flies is comparable to the number of time the behavior cassette rotates. This result shows that CS flies climb for approximately one track with every rotation of the cassette.

Duration of track. Once a fly initiated climbing, the duration of the track was measured. This is a measure of the fly's ability to sustain climbing. In the first minute, mean track duration for wild-type flies was 3.55 ± 0.33 s, which did not vary significantly even after the fly spent more time in the arena (Fig. 2*B′* and Dataset S1). Overall, wild-type flies spent 3.41 ± 0.28 s per track (Fig. 2*B* and Dataset S1). The mean track duration for wild-type flies never exceeded 10 s, suggesting that 15 s is sufficient for a fly to climb in the arena.

Total distance traveled. Next, we determined the overall locomotor ability of a fly, by calculating total distance traveled by the fly. Using BLU as the basic unit for distance measurements, total distance traveled for each fly was normalized to the body length. In the first minute of introduction of the fly into the arena, CS flies traveled 77.85 ± 4.48 BLUs, which did not vary much with the amount of time spent by the fly in the arena (Fig. 2*C′* and Dataset S1). In 5 min, on an average a fly walked a total distance of 363.99 ± 9.04 BLUs (Fig. 2*C* and Dataset S1).

Average speed. Instantaneous speed of the fly was determined by measuring the distance traveled by the fly between 2 consecutive frames. Subsequently, mean speed of a fly in one track was taken as the mean of instantaneous speeds of that track. For one fly, average speed was calculated by taking the mean speed from the speed of each track of that fly. Further, for a given genotype, the average speed was calculated by taking mean of the mean speed

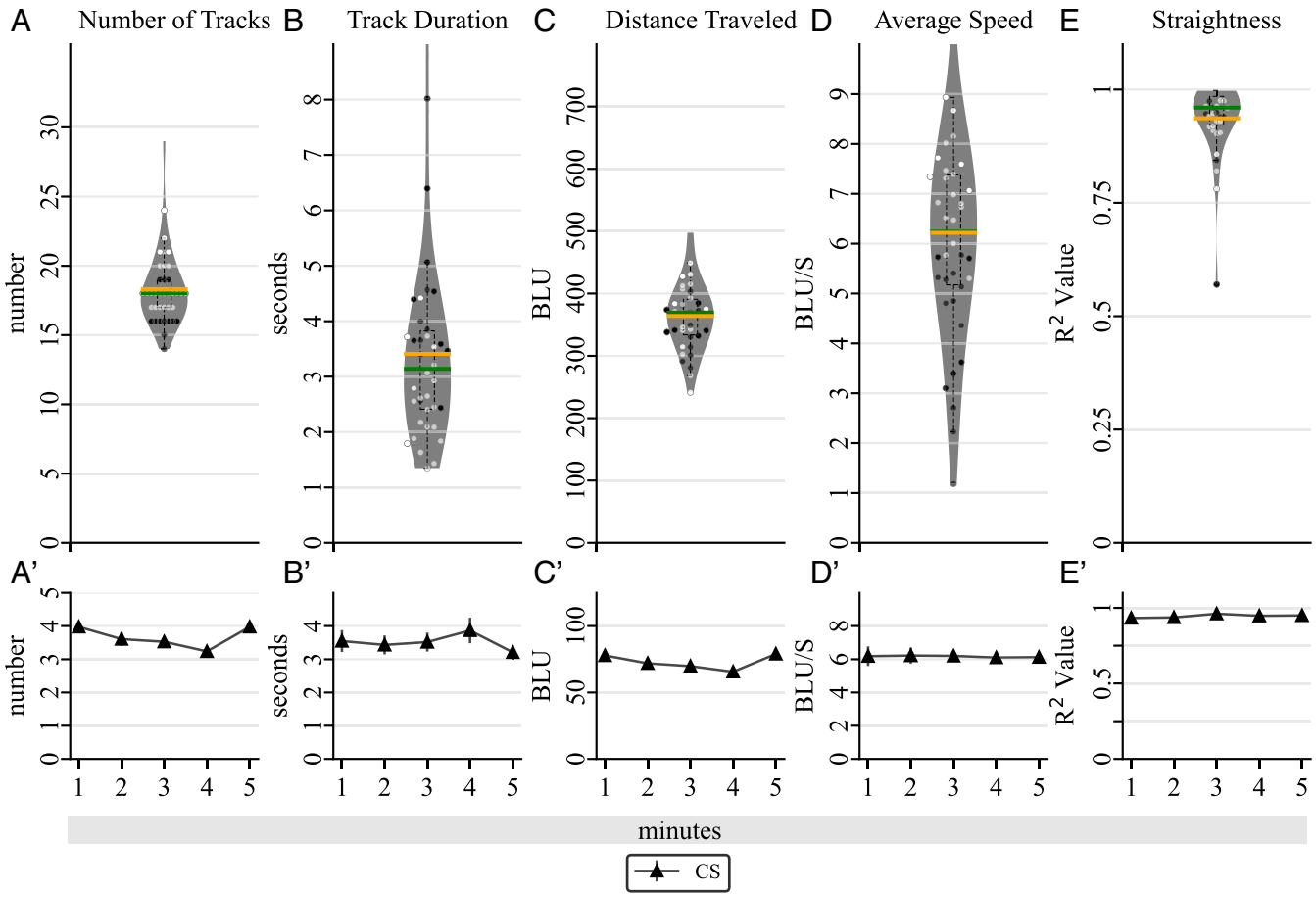

Fig. 2. Quantification of general climbing parameters of CS flies. (*A*) Average number of tracks. (*B*) Average duration of track. (*C*) Total distance. (*D*) Average speed of the fly in climbing. (*E*) Average path straightness for the paths climbed by the fly, represented by open and closed circles for males and females, respectively. (*A′*–*E′*) Time series analysis of each parameter in *A*–E, respectively. CS flies on an average climbed 18.32 ± 0.44 tracks (*A*) with mean track duration of 3.41 ± 0.28 s (*B*) and covered a total distance of 363.99 ± 9.04 BLUs (*C*) with an average speed of 6.22 ± 0.38 BLUs per s (*D*). The average path straightness was 0.94 ± 0.01 (*E*). The values on per-minute analysis did not change much with increase in time spent in the assay (Dataset S1). CS: $n > 15$ for both males and females. The colored area represents the range of full datasets, with mean represented as the orange line and median represented by the green line. Width of the colored plot indicates of the density of data points. The box inside the colored area corresponds to the data within *q1* and *q3*; the extended dotted line represents the data within (*q1* − 1.5 × IQR): (*q3* + 1.5 × IQR) range, where *q*1 and *q*3 are the first and third quartile, respectively; IQR: *q*3–*q*1 is the interquartile range.

from each fly. For the first minute, CS flies moved with a speed of 6.19 ± 0.60 BLUs per s and moved with the similar speeds beyond first minute into the arena (Fig. 2*D′* and Dataset S1). Overall, the mean speed of CS flies over 5 min was found to be 6.22 ± 0.38 BLUs per s (Fig. 2*D* and Dataset S1).

Track straightness. Finally, we calculated the straightness of the path traversed by the fly which is a measure of gross motor control and body orientation. Track straightness is calculated by drawing a regression model of the track and calculating the coefficient of determination, r^2, for that regression model. The value of r^2 indicates the track straightness; a higher r^2 value correlates to a straighter track. Average track straightness of a fly is calculated by taking the mean r^2 for all paths traversed by that fly. For wild-type flies, average track straightness for the first minute into the assay was 0.93 ± 0.02 and was similar for tracks climbed by the fly in the later minutes (Fig. 2*E′* and Dataset S1). The average track straightness for all of the paths climbed by the fly in 5 min was 0.94 ± 0.01 (Fig. 2*E* and Dataset S1).

Sexually dimorphic climbing behavior parameters. Locomotor differences within the population, based on the sex of the flies, were also characterized for the climbing parameters (males and females represented as open and closed circles, respectively, in Fig. 2). Although the number of tracks for wild-type females were slightly lower than for the wild-type males (17.69 ± 0.83, 18.77 ± 0.45, P = 0.02, Mann–Whitney U test; Fig. 2*A*), the average track duration of females was significantly higher than of males (4.58 ± 0.49, 2.56 ± 0.17, $P < 0.0001$, Mann–Whitney U test; Fig. 2*B*). The total distance covered by female wild-type flies was similar to males (344.05 ± 8.88 BLUs, 378.50 ± 13.56 BLUs, P = 0.059, unpaired t test; Fig. 2*C* and Dataset S2), but the average speed of females was significantly lower than males (4.29 ± 0.35 BLUs per s, 7.62 ± 0.38 BLUs per s, $P < 0.0001$, Mann–Whitney U test; Fig. 2*D*). The path straightness of females was similar to that of males (0.94 ± 0.03, 0.93 ± 0.01, P = 0.07, Mann–Whitney U test; Fig. 2*E* and Dataset S2). Finally, per-minute analysis reveals that females consistently have higher track duration and lower average speed as compared to wild-type males (Dataset S2). These data suggest that inherently climbing in female wild-type flies is slower than male wild-type flies but are similar for various other climbing parameters characterized.

Locomotion Parameters of Climbing w^{1118} Flies (White-Eyed Flies). Next, we compared the locomotion parameters of climbing wild-type CS flies to those of w^{1118} flies. White-eyed, w^{1118}, flies represent one of the most common genetic backgrounds for mutants and transgenic studies. Moreover, since they provide the genetic background for the mutants characterized below, they serve as controls for these mutants.

These control, w^{1118} flies showed a similar number of tracks as compared to the CS flies in total 5 min (18.32 ± 0.44, 16.46 ± 0.91, P = 0.17, Mann–Whitney U test; *SI Appendix*, Fig. S2*A*) and time series analysis also did not show any significant differences (Dataset S1 and *SI Appendix*, Fig. S2*A′*). The average track duration of w^{1118} flies was found to be significantly higher as compared to CS flies in total 5 min (4.24 ± 0.27 s, 3.41 ± 0.28 s, P = 0.003, Mann–Whitney U test; *SI Appendix*, Fig. S2*B*), although per-minute analysis revealed the difference in track duration to be different only in first 3 min (Dataset S1 and *SI Appendix*, Fig. S2*B′*). Both w^{1118} and CS flies traveled similar amount of distance in total 5 min (371.42 ± 22.45 BLUs, 363.99 ± 9.04 BLUs, P = 0.76, unpaired t test; *SI Appendix*, Fig. S1*C* and Dataset S1) and per-minute behavior (Dataset S1 and *SI Appendix*, Fig. S2*C′*). Average speed of w^{1118} flies, as compared to CS flies was less in overall 5 min behavior (4.86 ± 0.23 BLUs per s, 6.22 ± 0.38 BLUs per s, P = 0.001, unpaired t test; *SI Appendix*, Fig. S2*D*), as well as in per-minute behavior (Dataset S1 and *SI Appendix*, Fig. S2*D′*). Finally, the track straightness of w^{1118}, as compared to the CS flies, was low (0.85 ± 0.01, 0.94 ± 0.01, $P < 0.0001$, Mann–Whitney U test; *SI Appendix*, Fig. S2*E*) and per-minute analysis indicate that the track straightness in w^{1118} flies remains lower than the CS flies at every minute (Dataset S1 and *SI Appendix*, Fig. S2*E′*).

The data showed significant differences in track duration, average speed, and path straightness for CS wild-type flies and w^{1118} flies, thus emphasizing the role of genetic background in determining the behavior of different transgenic flies.

Locomotor Parameters of Heterozygous Mutants in Genes Implicated in the Fly PD Model. Although current assays for locomotor behavior in *Drosophila* measure climbing parameters reasonably well (8, 10), it is possible that detection of more subtle changes in climbing behavior might be important to understand the manifestation of locomotor disorders. To investigate this, we next studied the parameters of climbing behavior for several heterozygous mutants in genes implicated in the fly PD model. Climbing behavior parameters of control w^{1118} flies were compared to those of $PINK1^{RV}$, $park^{25}$/+, $LRRK^{ex1}$/+, and $LRRK^{ex1}/park^{25}$ flies for behavioral differences.

First, we compared the $PINK1^{RV}$ and $park^{25}$/+ flies with the controls. The total number of tracks climbed by both $PINK1^{RV}$ and $park^{25}$/+ flies were comparable to the controls in total 5 min (15.85 ± 0.85, 19.34 ± 0.96, 17.62 ± 1.08, P = 0.24, P = 0.27, Kruskal–Wallis test; Fig. 3*A*) and for per-minute data (Dataset S3 and Fig. 3*A′*). Track duration for $PINK1^{RV}$ and $park^{25}$/+ flies was also comparable to controls for total 5 min (3.36 ± 0.19 s, 3.61 ± 0.22 s, 3.77 ± 0.19 s, P = 0.38, P = 0.70, Kruskal–Wallis test; Fig. 3*B*) and for per-minute data (Dataset S3 and Fig. 3*B′*). Total distance traveled by $PINK1^{RV}$ was slightly less, whereas it was comparable to the controls for $park^{25}$/+ flies, in 5 min (286.31 ± 23.00 BLUs, 425.43 ± 26.50 BLUs, 387.87 ± 29.06 BLUs, P = 0.049, P = 0.48, one-way ANOVA; Fig. 3*C*). The time-series analysis showed that the total distance traveled by $PINK1^{RV}$ and $park^{25}$/+ flies was always comparable to the controls. (Dataset S3 and Fig. 3*C′*). Average speed of $PINK1^{RV}$ and $park^{25}$/+ flies was again comparable to the controls for total 5 min (4.43 ± 0.37 BLUs per s, 5.32 ± 0.39 BLUs per s, 4.93 ± 0.28 BLUs per s, P = 0.07, P = 0.67, Kruskal–Wallis test; Fig. 3*D*) and for per-minute data (Dataset S3 and Fig. 3*D′*). Both $PINK1^{RV}$ and $park^{25}$/+ did not deviate much from their track, showing track straightness similar to that of the controls for total 5-min data (0.86 ± 0.01, 0.85 ± 0.02, 0.86 ± 0.02, P = 0.89, P = 0.83, Kruskal–Wallis test; Fig. 3*E*) and for per-minute data (Dataset S3 and Fig. 3*E′*).

Next, we checked the climbing ability $LRRK^{ex1}$/+ and $LRRK^{ex1}/park^{25}$ flies. As compared to controls, both $LRRK^{ex1}$/+ and $LRRK^{ex1}/park^{25}$ flies climbed a significantly lower number of tracks in total 5 min (11.88 ± 0.91, 6.71 ± 0.90, 17.62 ± 1.08, P = 0.001, $P < 0.0001$, Kruskal–Wallis test; Fig. 3*A*) and per-minute analysis indicated that $LRRK^{ex1}/park^{25}$ flies show a time-dependent sharp decrease in number of tracks climbed (Dataset S3 and Fig. 3*A′*). Track duration for $LRRK^{ex1}$/+ and $LRRK^{ex1}/park^{25}$ flies was comparable to the controls in total 5 min (3.18 ± 0.26, 2.92 ± 0.42, 3.77 ± 0.19, P = 0.22, P = 0.06, Kruskal–Wallis test; Fig. 3*B*); however, per-minute analysis showed that track duration of $LRRK^{ex1}/park^{25}$ flies decrease soon after the first minute into the assay (Dataset S3 and Fig. 3*B′*). The total distance traveled by both genotypes in 5 min was significantly less than the controls (176.10 ± 17.90 BLUs, 82.42 ± 10.85 BLUs, 387.87 ± 29.06 BLUs, $P < 0.0001$, $P < 0.0001$, Kruskal–Wallis test; Fig. 3*C*) and similarly per-minute analysis showed flies from both genotypes climbing less distance than controls at every minute (Dataset S3 and Fig. 3*C′*). Again, the average speed of $LRRK^{ex1}$/+ and $LRRK^{ex1}/park^{25}$ flies was lower in comparison to the controls (4.41 ± 1.00 BLUs per s, 2.96 ± 0.27 BLUs per s, 4.94 ± 0.28 BLUs per s, Kruskal–Wallis test; Fig. 3*D*). The per-minute analysis also showed that the average speed was always lower than the controls for both $LRRK^{ex1}$/+ and $LRRK^{ex1}/park^{25}$ flies and decreased consistently for the

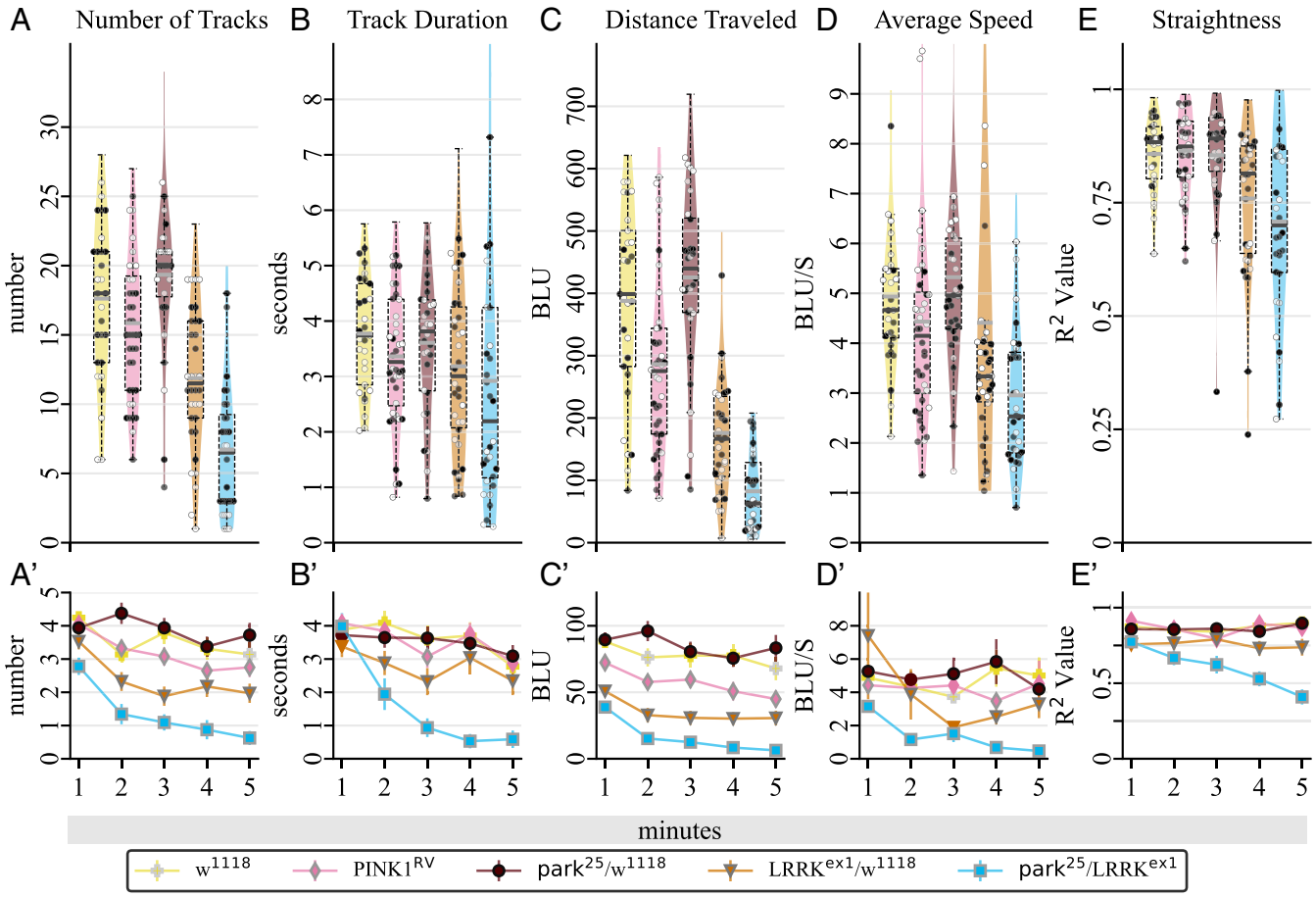

Fig. 3. (*A–E*) Quantification of various climbing parameters of Parkinson's mutants. In total 5 min, as compared to controls, LRRK^{ex1}/+ and LRRK^{ex1}/*park^{25}* flies climbed (*A*) a lesser number of paths (11.88 ± 0.91, 6.71 ± 0.90, 17.62 ± 1.08, $P = 0.001$, $P < 0.0001$, Kruskal–Wallis test) and (*C*) less distance (176.10 ± 17.90 BLUs, 82.42 ± 10.85 BLUs, 387.87 ± 29.06 BLUs, $P < 0.0001$, $P < 0.0001$, Kruskal–Wallis test). Average climbing speed of LRRK^{ex1}/*park^{25}* flies was significantly less than controls (2.96 ± 0.27 BLUs per s, 4.94 ± 0.28 BLUs per s, Kruskal–Wallis test). Per-minute analysis revealed that, with respect to controls, LRRK^{ex1}/+ and LRRK^{ex1}/*park^{25}* show a decreasing trend for all of the parameters with significantly low values after 1 min into the assay (Dataset S3). Climbing parameters of PINK1^{RV} and *park^{25}*/+ flies always remained similar to the controls (Dataset S3). w^{1118}: $n > 12$; LRRK^{ex1}/+: $n > 15$; LRRK^{ex1}/*park^{25}*: $n > 12$; *park^{25}*/+: $n > 15$; PINK1^{RV}: $n > 20$ for both males and females). Open and closed circles represent males and females, respectively. (*A′–E′*) Time series analysis of each parameter in *A–E*, respectively. Figure representation similar to Fig. 2.

LRRK^{ex1}/*park^{25}* flies (Dataset S3 and Fig. 3*D′*). Finally, track straightness of flies from both genotypes was similar to that of controls in 5 min (0.76 ± 0.03, 0.71 ± 0.04, 0.86 ± 0.02, $P = 0.03$, $P = 0.009$, Kruskal–Wallis test; Fig. 3*E*) and per-minute analysis revealed that the track straightness of LRRK^{ex1}/*park^{25}* flies decreased significantly after 2 min into the assay (Dataset S3 and Fig. 3*D′*).

Finally, we compared LRRK^{ex1}/+ and LRRK^{ex1}/*park^{25}* to measure the effect of *park^{25}* in LRRK^{ex1} background. As compared to LRRK^{ex1}/+, LRRK^{ex1}/*park^{25}* showed decrease in number of tracks (11.88 ± 0.91, 6.72 ± 0.90, $P = 0.0098$, Kruskal–Wallis test; Fig. 3*A*) and in total distance traveled (176.09 ± 17.891, 82.42 ± 10.85, $P = 0.008$, Kruskal–Wallis test; Fig. 3*C*). However, in per-minute analysis, as compared to LRRK^{ex1}/+, LRRK^{ex1}/*park^{25}* showed significant decrease in all parameters for climbing locomotor behavior after 3 min into the assay (Dataset S3 and Fig. 3 *A′–E′*).

Taken together, these findings indicate that, relative to controls, flies from genotypes having a mutation in the LRRK gene (i.e., LRRK^{ex1}/+ and LRRK^{ex1}/*park^{25}*) start showing severe locomotor deficits within a minute of introduction into the arena. The other 2 genotypes, *park^{25}*/+ and PINK1^{RV}, do not show any significant departure from controls. The locomotor defects in LRRK^{ex1}/+ seem to be exacerbated in the transheterozygote condition with *park^{25}* mutation. However, an understanding of the detailed interaction between mutations in the 2 genes requires further investigation.

Sexual Dimorphism in Climbing Behavior of PD Flies. Again, comparing data for total 5-min behavior between male and female flies of different PD mutants revealed differences for various climbing parameters. The males of w^{1118} flies, as compared to females of w^{1118}, climbed more number of tracks (19.33 ± 1.01, 15.32 ± 1.09, $P = 0.01$, unpaired *t* test; Dataset S2) with shorter track duration (3.48 ± 0.19 s, 4.72 ± 0.34 s, $P = 0.001$, Mann–Whitney *U* test; Dataset S2) and traveled more distance (441.22 ± 27.80 BLUs, 340.42 ± 26.86; Dataset S2) with greater speed (5.35 ± 0.26, 4.64 ± 0.32; Dataset S2). In PINK1^{RV} flies, males climbed more numbers of tracks than females (18.11 ± 1.36, 14.0 ± 0.93, $P = 0.14$, unpaired *t* test; Dataset S2) with greater distance (363.15 ± 37.79 BLUs, 223.44 ± 20.53 BLUs) and higher speed (5.17 ± 0.49 BLUs per s, 3.83 ± 0.51 BLUs per s). Males of *park^{25}*/+ showed greater climbing speed as compared to females (5.78 ± 0.57 BLUs per s, 4.87 ± 0.51 BLUs per s, $P = 0.009$, Mann–Whitney *U* test; Dataset S2). In LRRK^{ex1}/+ flies, males climbed a smaller number of tracks as compared to females (9.75 ± 1.47, 13.78 ± 0.93, $P = 0.024$, unpaired *t* test; Dataset S2) while showing greater track straightness than females (0.81 ± 0.03, 0.72 ± 0.04, $P = 0.047$,

Mann–Whitney U test; Dataset S2). Finally, in LRRK^{ex1}/*park*^{25} flies, as compared to females males climbed a smaller number of tracks (3.46 ± 0.70, 8.95 ± 1.20, $P = 0.002$, unpaired t test; Dataset S2).

These data suggested that the differences in various parameters of climbing behavior of males and females in PD mutants is still there despite the mutations in various genes related to PD.

Gait Pattern of Heterozygous Mutants in Genes Implicated in the Fly PD Model. To further investigate the differences in locomotor behavior, gait pattern of the flies showing significant deviations from the controls was measured. We measured gait pattern of w^{1118}, LRRK^{ex1}/+, and LRRK^{ex1}/*park*^{25} flies using percent concurrency, swing amplitude, stance amplitude, swing duration, and stance duration. The S3 concurrency percentage, the amount of time when the legs move in a tripod gait, of the LRRK^{ex1}/*park*^{25} flies was significantly lower than control and LRRK^{ex1}/+ flies (23.25 ± 4.11%, 40.81 ± 4.0%, 31.39 ± 2.47%, $P < 0.0001$, $P = 0.003$; Dataset S4 and Fig. 4*A*) whereas LRRK^{ex1}/+ flies did not show any change in S3 concurrency as compared to the controls ($P = 0.12$). Further, the percent of time the flies moved only one leg (i.e., the S1 concurrency percentage) was higher in the LRRK^{ex1}/*park*^{25} transheterozygous flies as compared to the controls and heterozygous LRRK^{ex1}/+ flies (38.46 ± 3.09%, 24.62 ± 2.31%, 31.28 ± 1.99%, $P = 0.0004$, $P = 0.058$; Dataset S4 and Fig. 4*A*) and LRRK^{ex1}/+ flies did not show any difference as compared to the controls in S1 state ($P = 0.069$). The LRRK^{ex1}/*park*^{25} flies climbed slowly as compared to the control and LRRK^{ex1}/+ flies (12.44 ± 0.60 mm/s, 17.93 ± 0.61 mm/s, $P < 0.0001$, 17.95 ± 0.63 mm/s, $P < 0.0001$; Dataset S4) in the tracks analyzed for gait (Fig. 4*B*). The

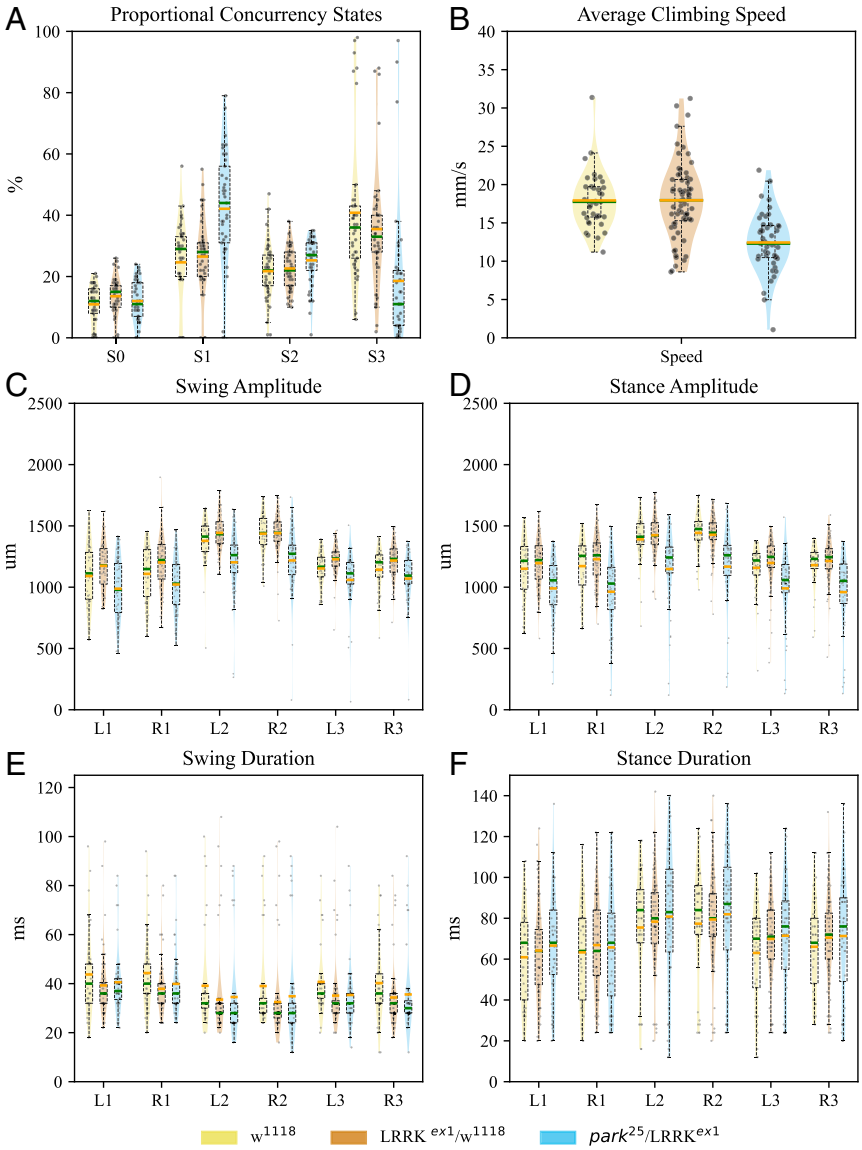

Fig. 4. Gait quantification in climbing Parkinson's flies. The leg concurrency of LRRK^{ex1}/*park*^{25} flies in S1 state was higher (38.45 ± 3.09%) whereas in the S3 state was lower (23.25 ± 4.1%) as compared to the w^{1118} (S1: 24.62 ± 2.30%, $P = 0.0004$; S3: 40.81 ± 4.0%, $P < 0.0001$) and LRRK^{ex1}/+ (S1: 31.28 ± 1.99%, $P = 0.058$; S3: 31.39 ± 2.47%, $P = 0.003$) flies (*A*). The LRRK^{ex1}/*park*^{25} flies showed lower climbing speed as compared to the control and LRRK^{ex1}/+ flies (12.44 ± 0.60 BLUs per s, 17.93 ± 0.61 BLUs per s, $P < 0.0001$, 17.95 ± 0.63 BLUs per s, $P < 0.0001$) in the tracks analyzed for gait (*B*). The swing amplitude of LRRK^{ex1}/*park*^{25} was lower for L2 and R2 legs as compared to the controls ($P = 0.0001$, $P < 0.0001$) and for all 3 pairs of LRRK^{ex1}/+ flies ($P \leq 0.0001$, *C*, S3). The stance amplitude of LRRK^{ex1}/*park*^{25} flies was lower for all legs as compared to control and LRRK^{ex1}/+ flies ($P \leq 0.01$, *D*, S3). The swing duration of T1 and T2 leg pairs of LRRK^{ex1}/*park*^{25} flies was lower than controls ($P \leq 0.03$, *E*, S3). The stance duration for all legs of all genotypes was similar (*F*). w^{1118}: $n = 37$; LRRK^{ex1}/+: $n = 64$; LRRK^{ex1}/*park*^{25}: $n = 44$. Figure representation similar to Fig. 2.

swing amplitude of LRRK^{ex1}/*park*^{25} was lower than that of controls for L2 (1,202.70 ± 41.18 μm, 1,378.0 ± 33.67 μm, $P = 0.0001$; *SI Appendix*, Table S3 and Fig. 4*C*) and R2 legs (1,218.10 ± 41.92 μm, 1,436.67 ± 27.21 μm, $P < 0.0001$; Dataset S4 and Fig. 4*C*) and for all legs of LRRK^{ex1}/+ flies ($P \leq 0.0001$; Dataset S4 and Fig. 4*C*). The stance amplitude of LRRK^{ex1}/*park*^{25} flies was lower for all legs as compared to control and LRRK^{ex1}/+ flies ($P \leq 0.01$; Dataset S4 and Fig. 4*D*). The swing duration of prothoracic and mesothoracic legs of LRRK^{ex1}/*park*^{25} and LRRK^{ex1}/+ flies was lower than controls ($P \leq 0.03$; Dataset S4 and Fig. 4*E*). The stance duration for all legs of all genotypes was comparable (Dataset S4 and Fig. 4*F*).

The data from the gait analysis of the flies show severe limb movement defects in the flies with deficits in overall locomotion in the body-centric analysis and hence provide further insights into the behavioral factors leading to defective locomotion in LRRK^{ex1}/+ and LRRK^{ex1}/*park*^{25} flies.

Locomotor Parameters in a Proprioceptive Mutant. Finally, we investigated the climbing locomotor defects that result from a homozygous proprioceptory mutation (*Trp-γ*^{1}) known to exclusively affect fine motor control in *Drosophila* (3). Previous studies indicate that *Trp-γ*^{1} flies have fine motor control defects in locomotion but not any gross motor defect. Thus, overall locomotion in *Trp-γ*^{1} flies is not affected much, but large gap crossing is highly impaired (3). We hypothesized that fine motor coordination might be important for climbing. Hence, to further understand the role of proprioceptive neurons expressing *Trp-γ* in motor coordination, we studied climbing of *Trp-γ*^{1} flies in greater depth.

Analysis of climbing behavior of *Trp-γ*^{1} flies for a total of the first 5 min into the assay showed that, as compared to controls, these flies climbed more tracks (23.78 ± 1.27, 17.53 ± 0.79, $P < 0.0001$, Mann–Whitney *U* test; Fig. 5*A*) with a lower average duration of tracks (3.24 ± 0.35 s, 4.04 ± 0.20 s, $P < 0.0001$, Mann–Whitney *U* test; Fig. 5*B*) and traveled a longer distance (524.77 ± 34.22 BLUs, 395.97 ± 20.61 BLUs, $P = 0.001$, unpaired *t* test; Fig. 5*C*) with a greater average speed (6.71 ± 0.52 BLUs per s, 5.03 ± 0.21 BLUs per s, $P = 0.001$, Mann–Whitney *U* test; Fig. 5*D*). Track straightness of *Trp-γ*^{1} flies was similar to the controls in total 5 min (0.88 ± 0.01, 0.86 ± 0.01, unpaired *t* test; Fig. 5*E*). Time-series analysis also revealed that, compared to controls, *Trp-γ*^{1} flies consistently climbed a greater number of tracks, had less average track duration, climbed more distance, and had greater speed (Dataset S5 and Fig. 5 *A′*–*E′*).

These results indicate that *Trp-γ*^{1} flies have higher motility and higher speeds as compared to the controls while climbing. As *Trp-γ* is expressed in femoral chordotonal organs, it is possible that during climbing precise leg position control is impaired. A detailed gait analysis during climbing in *Trp-γ*^{1} flies would be important to understand the role of *Trp-γ* in climbing further.

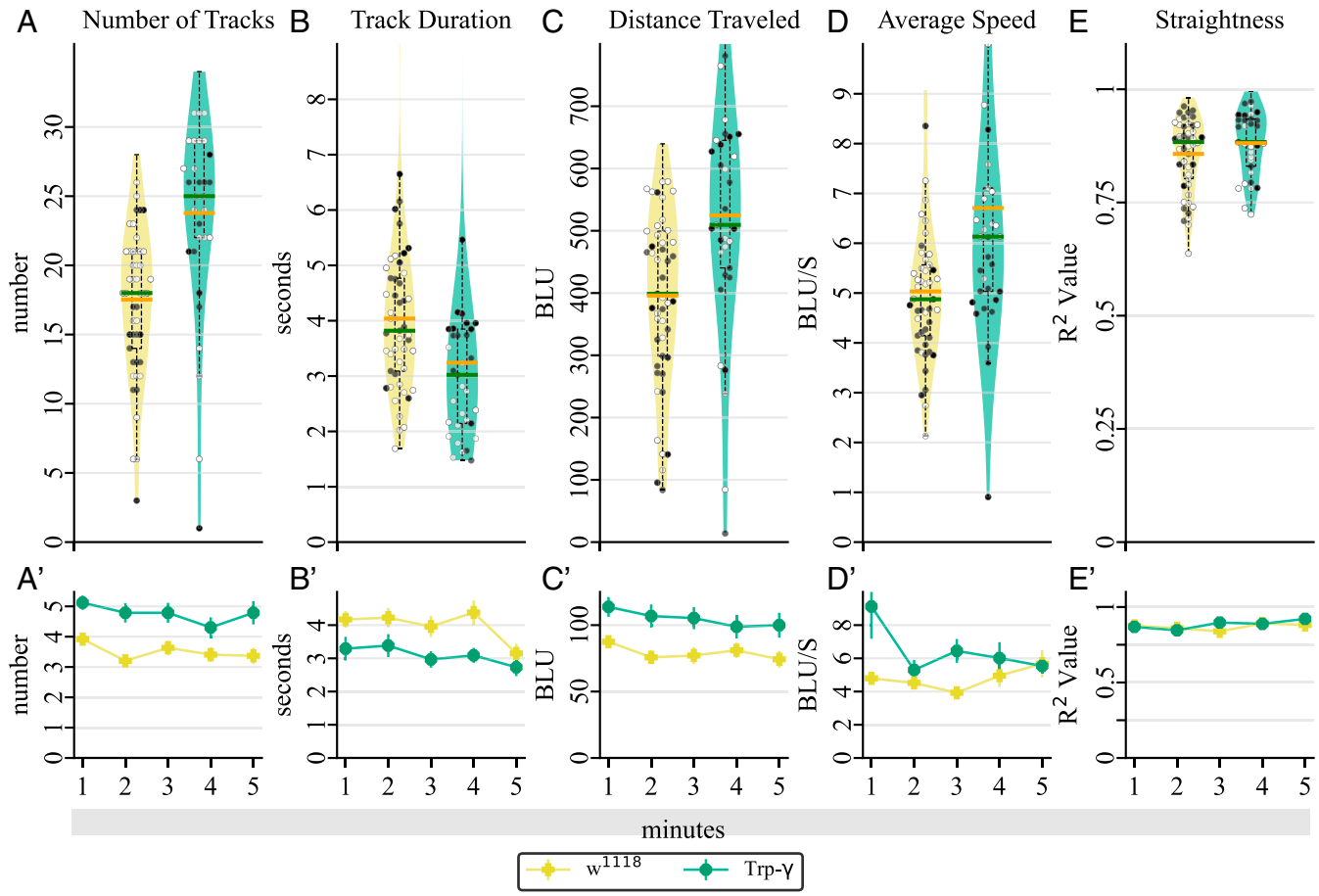

Fig. 5. Quantification of various climbing parameters of Trp-γ mutants. In total 5 min, as compared to controls, Trp-γ flies climb (*A*) more number of paths (23.78 ± 1.27, 17.53 ± 0.79, $P < 0.0001$, Mann–Whitney *U* test), (*B*) for shorter duration (3.24 ± 0.35 s, 4.04 ± 0.20 s, $P < 0.0001$, Mann–Whitney *U* test), (*C*) more distance (524.77 ± 34.22 BLUs, 395.97 ± 20.61 BLUs, $P = 0.001$, unpaired *t* test), and (*D*) faster (6.71 ± 0.52 BLUs per s, 5.03 ± 0.21 BLUs per s, $P = 0.001$, Mann–Whitney *U* test; Dataset S5). Per-minute analysis reveal that, with respect to controls, Trp-γ flies consistently show (*A′*) more number of tracks, (*B′*) with lower average track duration, and (*C′*) climbed more distance with (*D′*) greater speed (Dataset S5). Genotype: Trp-γ:w^{-};;Trp-γ^{1} . w^{1118}: $n > 18$; Trp-γ: $n > 15$, for both males and females). Open and closed circles represent males and females, respectively. (*A′*–*E′*) Time series analysis of each parameter in *A*–E, respectively. Figure representation similar to Fig. 2.

GTI: A Measure of Graviception in Flies. Flies have an innate tendency to climb against gravity. To measure a fly's response to gravity in our climbing assay, we introduce GTI, a measure of a fly's ability to sense and respond to gravity during locomotion. GTI is defined as the sum total of score of all tracks scored for their direction of motion apropos of gravity divided by the total number of tracks climbed by the fly (Fig. 6*B*). A track is scored −1 if it shows an ascending climb (T_{up}), scored +1 if it shows a descending climb (T_{Down}), and scored zero if it shows displacement less than 1 BLU in vertical direction (T_{zero}, Fig. 6*A*). Thus, a negative GTI indicates that the fly is negatively geotactic and a positive GTI represents a positively geotatic fly.

The wild-type flies showed a highly negative (−0.93 ± 0.02; Fig. 6*C*) GTI in total 5 min into the assay. Also, per-minute analysis showed that GTI for wild-type flies does not vary with respect to time (Dataset S5 and Fig. 6*C′*). The white-eyed, w^{1118}, flies showed less negative GTI as compared to the CS flies in total 5 min (−0.54 ± 0.07, $P < 0.0001$, Mann–Whitney *U* test; Fig. 6*C*) and the GTI increased in the last minute of the assay (Dataset S5 and Fig. 6*C′*). *Trp-γ*^{1} flies showed a significant increase in GTI, as compared to controls (−0.21 ± 0.06, −0.43 ± 0.06, $P = 0.027$, Kruskal–Wallis test; Fig. 6*C*) for total 5 min.

Next, we segregated the negatively and positively geotactic tracks within each genotype and compared their data for total 5 min of behavior recorded. In CS flies, negative GTI tracks, as compared to the positive GTI tracks, showed higher number of tracks (17.63 ± 0.27, 1.92 ± 0.47, $P < 0.0001$, Mann–Whitney *U* test; Dataset S2) with greater track duration (3.45 ± 0.27 s, 1.90 ± 0.41 s, $P < 0.0001$, Mann–Whitney *U* test; Dataset S2) and covered more distance (351.94 ± 8.09 BLUs, 35.09 ± 7.52 BLUs, $P < 0.0001$, unpaired *t* test; Dataset S2) with even lower speed (6.05 ± 0.31 BLUs per s, 14.50 ± 7.67 BLUs per s, $P = 0.13$, Mann–Whitney *U* test; Dataset S2) and higher track straightness (0.95 ± 0.01, 0.33 ± 0.08, $P < 0.0001$, Mann–Whitney *U* test). Similarly, in w^{1118} flies also there were significant differences in climbing behavior for tracks with negative GTI and positive GTI. Negative GTI tracks, as compared to the positive GTI tracks of w^{1118} flies, were greater in number (12.85 ± 0.68, 5.26 ± 0.55, $P < 0.0001$, Mann–Whitney *U* test; Dataset S2) with greater track duration (4.57 ± 0.24, 2.90 ± 0.16, $P < 0.0001$, Mann–Whitney *U* test; Dataset S2) and covered more total distance (290.58 ± 18.0, 117.94 ± 14.77, $P < 0.0001$, Mann–Whitney *U* test; Dataset S2) with greater track straightness (0.87 ± 0.02, 0.76 ± 0.03, $P = 0.004$, Mann–Whitney *U* test; Dataset S2). However, in Trp-*γ*^{1} flies, negatively geotactic tracks differed from positively geotactic tracks in number of tracks (14.09 ± 0.94, 10.32 ± 0.74, $P = 0.003$, unpaired *t* test; Dataset S2) and straightness (0.910 ± 0.01, 0.81 ± 0.03, $P < 0.0001$, Mann–Whitney *U* test; Dataset S2) only.

Overall, these data indicate that a differential response of flies to gravity can be quantified by GTI. Moreover, the results suggest that proprioceptory neurons expressing *Trp-γ* could be involved in the graviception response in flies.

Discussion

Climbing behavior in flies has been extensively studied for gross locomotor defects. Widely used climbing behavior assays employ mechanical startle as a way to induce locomotion in flies. Although highly effective, physical agitation of flies is an aggressive way to induce locomotion in flies. Physical agitation is liable to incorporate undesirable behavioral phenotypes in a fly's innate climbing response and mask subtle phenotypes. Also, automating the data collection and analysis could help mitigate the inconsistencies of this traditionally manual, labor intensive task. Therefore, we developed an assay to assess climbing ability of flies which hinges upon the fly's innate response to gravity, that is, negative geotaxis, during climbing. An automated behavioral setup along with robust image analysis is particularly useful in high throughput of this assay.

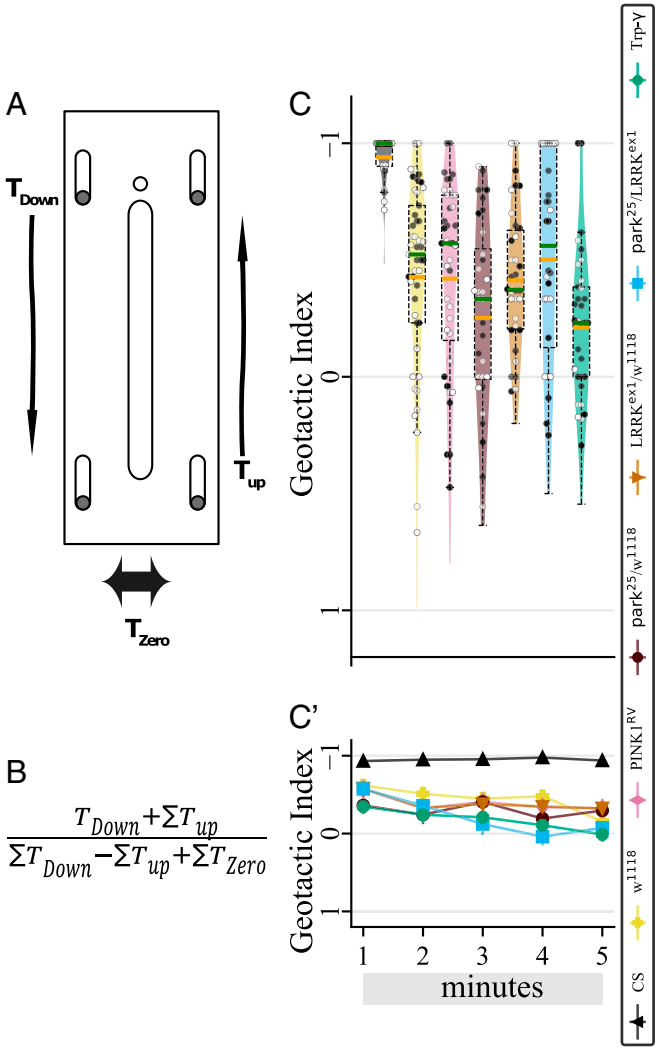

Fig. 6. GTI. (*A*) Schematic for GTI measurement. (*B*) Function for GTI calculation. (*C*) The GTI of all transgenic flies is lower than CS ($P < 0.0001$ for all genotypes, Kruskal–Wallis test) in the total 5 min (Dataset S6). (*C′*) Per-minute calculations show GTI of LRRK^{ex1}/+, LRRK^{ex1}/*park*^{25} and Trp-γ flies was consistently lower than CS and control flies (Dataset S6) (w^{1118}: $n > 18$; Trp-γ: $n > 15$, for both males and females). Figure representation similar to Fig. 2.

Computational tools for automated analysis of behavior of flies have been developed for over a decade and range from tools for simplistic tracking of flies, similar to one presented here (19), to more sophisticated machine learning-based behavior annotation tools (23, 24). Some of these tools specific for fly limb tracking have greatly contributed to our understanding of fly locomotion at the level of individual leg control (20, 25–27). However, technical challenges of current methods limit our ability to quickly screen through large numbers of freely moving flies over long distances. Our assay, along with being highly cost-effective, mitigates these issues and complements the limb-tracking methods already available in the field for understanding various important factors such as fatigue and GTI. Current techniques to analyze climbing do not pick up these subtle parameters, which could provide crucial insights into the neural mechanisms behind manifestations of different neuromuscular disorders. Using this assay, one can quickly screen through large number of flies for gross locomotor defects and can employ the same apparatus for fine-scale gait analysis to further narrow down potential hits.

Although this assay could provide information on some aspects of the fly's climbing ability in a manner similar to previously used methods, it is important to note that substantially more information can be gained over previously used methods (Fig. 2). In this study, we describe parameters to characterize details of a fly's climbing behavior (Fig. 2 *A*–*E*), along with a detailed temporal analysis of these parameters (Fig. 2 *A′*–*E′*). Our fine-temporal analysis enables an understanding of climbing dynamics in accordance with the time spent in the arena. Flexibility in image and data analysis software allows further extraction of various previously undescribed, but important, parameters from climbing data.

In addition to studying wild-type flies, we also characterized climbing behavior in various fly mutant lines related to PD, viz. $park^{25}$ and $LRRK^{ex1}$, and $PINK1^{RV}$, a revertant allele for PINK1 (15), and controls such as w^{1118}, a genotype commonly used for generation of transgenics. Both the *parkin* and PINK1 genes are implicated in PD, and although mutations in *parkin* and PINK1 are known be autosomal-recessive, heterozygous mutations in these genes are thought to enhance the risk for PD early onset (13). In addition to using the $park^{25}$/+ and $LRRK^{ex1}$/+ flies to test climbing specifically in heterozygous state, we also studied $LRRK^{ex1}/park^{25}$ transheterozygous flies to explore the possibility of using this assay for studying novel interactors in various neurodegenerative diseases. Comparing $LRRK^{ex1}/park^{25}$ with $park^{25}$/+, $LRRK^{ex1}$/+, and $PINK1^{RV}$, we found that $LRRK^{ex1}/park^{25}$ flies show significantly reduced mobility within a minute, replicating aspects of the clinically observable bradykinesia phenotype in PD patients. Furthermore, the gait analysis of $LRRK^{ex1}$/+ and $LRRK^{ex1}/park^{25}$ flies indicated that limb movements in the LRKK–*parkin* transheterozygote flies are severely compromised. A recent study showed defective hind limb movement in other PD mutants in a smaller arena (28). However, in our study flies show significant defects in all 3 limb pairs which could be due to unconstraint movement in a larger arena. Presence of $park^{25}$ mutation in conjunction with $LRRK^{ex1}$ mutation exacerbates the locomotor defects in fly PD model, suggesting putative interactions between autosomal-dominant and -recessive alleles of genes implicated in the juvenile and late-onset PD model. A detailed investigation of this possible genetic interaction could be important for understanding the manifestation of more complicated forms of PD. Taken together, the high parametric resolution analysis of climbing behavior presented here helps in dissecting the possible locomotor defects of these fly mutants.

We also characterized a fly proprioceptive mutant, $Trp\text{-}\gamma^{1}$, for gravitaxis impairment. *Trp-γ*, a TRPC channel (29), is known to be expressed in thoracic bristles and femoral chordotonal organs and $Trp\text{-}\gamma^{1}$ mutants show only fine motor control defects (3). Interestingly, these flies manifested numerous descending tracks along with the ascending tracks, which was not attributed to less overall movement of these flies. This prompted us to investigate the geotactic ability of these mutants. To do so, we introduced the GTI as a way to measure a fly's response to gravity during locomotion. Graviception in flies plays an important role in vertical climbing of flies, and the GTI provides a way to measure and assess the innate geotactic response of the fly. Wild-type *Drosophila* are highly sensitive to gravity and show a strong negative geotactic response to gravity while climbing. Negative geotaxis in *Drosophila* is mediated by *TRPA* genes *pyrexia* and *painless* (30), but a role of a TRPC channel, *Trp-γ*, in gravity sensing was unknown. We found that the GTI of $Trp\text{-}\gamma^{1}$ mutant flies was less negative. Data from our study thus indicate a putative role of *Trp-γ* in graviception in *Drosophila* and warrant further studies.

In summary, we present a cost-effective assay for quantifying *Drosophila* climbing behavior at high parametric resolution. This assay differs from traditional climbing behavior assays by exploiting the innate negative geotactic behavior of flies rather than relying on physical agitation. It provides insight into various locomotor parameters which are important for a quantitative characterization of fly climbing. This assay, together with the open source data analysis software, opens up additional routes to extracting parameters relevant to varied experimental questions.

ACKNOWLEDGMENTS. We thank the *Drosophila* community and National Centre for Biological Sciences (NCBS) fly facility for the generous supply of fly strains. We thank Dhananjay Chaturvedi for helpful discussions and suggestions. We thank the mechanical and electrical workshop at NCBS for fabricating the components of the setup. A.A. was supported by the Council of Scientific and Industrial Research. This work was supported by National Centre for Biological Sciences – Tata Institute of Fundamental Research and a J. C. Bose fellowship to K.V.

1. C. S. Sherrington, *The Integrative Action of the Nervous System* (Charles Scribner's Sons, New York, 1906).
2. F. W. Carpenter, The reactions of the pomace fly (Drosophila ampelophila Loew) to light, gravity, and mechanical stimulation. *Am. Nat.* **39**, 157–171 (1905).
3. B. Akitake *et al*., Coordination and fine motor control depend on Drosophila TRPγ. *Nat. Commun.* **6**, 7288 (2015).
4. T. R. Jahn *et al*., Detection of early locomotor abnormalities in a Drosophila model of Alzheimer's disease. *J. Neurosci. Methods* **197**, 186–189 (2011).
5. M. B. Feany, W. W. Bender, A Drosophila model of Parkinson's disease. *Nature* **404**, 394–398 (2000).
6. J. W. Gargano, I. Martin, P. Bhandari, M. S. Grotewiel, Rapid iterative negative geotaxis (RING): A new method for assessing age-related locomotor decline in Drosophila. *Exp. Gerontol.* **40**, 386–395 (2005).
7. R. Borg, R. J. Cauchi, The Gemin associates of survival motor neuron are required for motor function in Drosophila. *PLoS One* **8**, e83878 (2013).
8. S. Benzer, Behavioral mutants of Drosophila isolated by countercurrent distribution. *Proc. Natl. Acad. Sci. U.S.A.* **58**, 1112–1119 (1967).
9. A. Barekat *et al*., Using Drosophila as an integrated model to study mild repetitive traumatic brain injury. *Sci. Rep.* **6**, 25252 (2016).
10. H. K. Inagaki, A. Kamikouchi, K. Ito, Methods for quantifying simple gravity sensing in Drosophila melanogaster. *Nat. Protoc.* **5**, 20–25 (2010).
11. F. W. Wolf, A. R. Rodan, L. T.-Y. Tsai, U. Heberlein, High-resolution analysis of ethanol-induced locomotor stimulation in Drosophila. *J. Neurosci.* **22**, 11035–11044 (2002).
12. J. Hirsch, Studies in experimental behavior genetics. II. Individual differences in geotaxis as a function of chromosome variations in synthesized Drosophila populations. *J. Comp. Physiol. Psychol.* **52**, 304–308 (1959).
13. O. Corti, S. Lesage, A. Brice, What genetics tells us about the causes and mechanisms of Parkinson's disease. *Physiol. Rev.* **91**, 1161–1218 (2011).
14. V. L. Hewitt, A. J. Whitworth, *Mechanisms of Parkinson's Disease: Lessons from Drosophila* (Elsevier Inc., ed. 1, 2017).
15. J. Park *et al*., Mitochondrial dysfunction in Drosophila PINK1 mutants is complemented by parkin. *Nature* **441**, 1157–1161 (2006).
16. J. C. Greene *et al*., Mitochondrial pathology and apoptotic muscle degeneration in Drosophila parkin mutants. *Proc. Natl. Acad. Sci. U.S.A.* **100**, 4078–4083 (2003).
17. A. Claridge-Chang *et al*., Writing memories with light-addressable reinforcement circuitry. *Cell* **139**, 405–415 (2009).
18. B. R. H. Geurten, P. Jähde, K. Corthals, M. C. Göpfert, Saccadic body turns in walking Drosophila. *Front. Behav. Neurosci.* **8**, 365 (2014).
19. K. Branson, A. A. Robie, J. Bender, P. Perona, M. H. Dickinson, High-throughput ethomics in large groups of Drosophila. *Nat. Methods* **6**, 451–457 (2009).
20. S. B. M. Gowda *et al*., GABAergic inhibition of leg motoneurons is required for normal walking behavior in freely moving *Drosophila*. *Proc. Natl. Acad. Sci. U.S.A.* **115**, E2115–E2124 (2018).
21. K. Noguchi, Y. R. Gel, E. Brunner, F. Konietschke, nparLD: An R software package for the nonparametric analysis of longitudinal data. *J. Stat. Softw.* **50**, 1–23 (2012).
22. F. Konietschke, M. Placzek, F. Schaarschmidt, L. A. Hothorn, nparcomp : An R software package for nonparametric multiple comparisons and simultaneous confidence intervals. *J. Stat. Softw.* **64**, 1–17 (2015).
23. A. A. Robie *et al*., Mapping the neural substrates of behavior. *Cell* **170**, 393–406.e28 (2017).
24. E. Eyjolfsdottir, K. Branson, Y. Yue, P. Perona, Learning recurrent representations for hierarchical behavior modeling. arXiv:1611.00094 (1 November 2016).
25. C. S. Mendes, I. Bartos, T. Akay, S. Márka, R. S. Mann, Quantification of gait parameters in freely walking wild type and sensory deprived Drosophila melanogaster. *eLife* **2**, e00231 (2013).
26. V. Uhlmann, P. Ramdya, R. Delgado-Gonzalo, R. Benton, M. Unser, FlyLimbTracker: An active contour based approach for leg segment tracking in unmarked, freely behaving Drosophila. *PLoS One* **12**, e0173433 (2017).
27. A. Isakov *et al*., Recovery of locomotion after injury in Drosophila melanogaster depends on proprioception. *J. Exp. Biol.* **219**, 1760–1771 (2016).
28. S. Wu *et al*., Fully automated leg tracking of Drosophila neurodegeneration models reveals distinct conserved movement signatures. *PLoS Biol.* **17**, e3000346 (2019).
29. X. Z. Xu, F. Chien, A. Butler, L. Salkoff, C. Montell, TRPgamma, a drosophila TRP-related subunit, forms a regulated cation channel with TRPL. *Neuron* **26**, 647–657 (2000).
30. Y. Sun *et al*., TRPA channels distinguish gravity sensing from hearing in Johnston's organ. *Proc. Natl. Acad. Sci. U.S.A.* **106**, 13606–13611 (2009).